Obtaining of films of tungsten trioxide (WO_3) by resistive heating of a tungsten filament

J. Díaz-Reyes
CIBA-IPN
Ex –Hacienda de San Juan Molino Km. 1.5. Tepetitla,
Tlaxcala. C. P. 90700. México.

V. Dorantes-García
Preparatoria "Simón Bolívar", BUAP
4 Oriente 408. Col. Centro. C.P. 74200. Atlixco, Pue. México

A. Pérez-Benítez
FCQ-BUAP
14 Sur y Av. San Claudio. Col. San Manuel. C. P. 72570
Puebla, Pue. México

J. A. Balderas-López
UPIBI-IPN
Av. Acueducto S/N, Col. Barrio la Laguna, C. P. 07340, México, D. F.
(Recibido: 15 de enero de 2008; Aceptado: 18 de marzo de 2008)

Thin film of tungsten oxide (WO_3) has been studied extensively as an electrochromic material and has numerous applications in electrochromic devices, smart windows, gas sensors and optical windows. In order to explore the possibility of using it in electrochromic devices, thorough study the optical properties of the WO_3 is an important step. The WO_3 layers have been grown by hot-filament metal oxide deposition technique under atmospheric pressure and an oxygen atmosphere. By FTIR and Raman scattering studies we found that the films contain hydrates. We have observed that the thin films of WO_3 can be satisfactorily grown by this technique.

Keywords: WO_3; Chemistry of light bulb; Infrared spectroscopy; Raman scattering

1. Introduction

There is a considerable interest in the research and development of materials and devices that can be used for optical switching of large-scale glazings. Several potential switching technologies are available for glazings, including those based on the electrochromism, thermochromism and photochromism phenomena. Tungsten oxide (WO_3) has been extensively studied and is reported to have interesting physical properties, which makes it suitable for electrochromic and a variety of potential applications [1]. These properties were first reported by Deb [2] and since then many theories have been proposed for the observed electrochromic mechanism in WO_3 [3]. The physical properties of a material are greatly affected by its structural order and morphology. Different preparation methods have their specific advantages in viewpoint of the film quality and production cost of materials for the different applications. Thin films of tungsten oxide have two extreme structural orders like amorphous (α-WO_3) and polycrystalline (c-WO_3). The structural configuration of the WO_3 crystal lattice is the distorted rhenium trioxide (ReO_3) structure [4]. Though the tungsten oxide was known as a promising candidate for electrochromic devices [5], it was not popular because of the fast developments in the liquid-crystal displays (LCDs). Tungsten oxide films are presently used in sunglasses and automotive rear-view mirrors, sun roofs, variable-tinted windows for automotive glass and building windows. Many researchers have built and tested whole electrochromic devices with promising results [6]. The WO_3 film is quite porous and smaller alkali ions can be easily intercalated and deintercalated into it. The density of the films starts to increase significantly up to a deposition temperature of 200 ºC, and up to a post annealing of 300 ºC [3]. Moreover, the electrochromic device performance of WO_3 films basically depends on their structural, surface morphological, compositional and optical properties. It is important that the improvement of materials properties requires a closer inspection of preparation conditions and also the above mentioned properties of the films. In this regard, a large number of techniques for preparing WO_3 films were employed [9]. Out of which the electron beam evaporation technique, one of the physical vapor deposition methods, has been considered largely for the growth of device quality thin films [8]. Indeed, a systematic characterization of the above mentioned properties is of great interest and is necessary to understand the electrochromic properties of the WO_3 films. Hence, in the present study we have investigated the structural, morphological and optical properties of electron beam evaporated WO_3 films and the effect of the substrates and annealing temperature on these

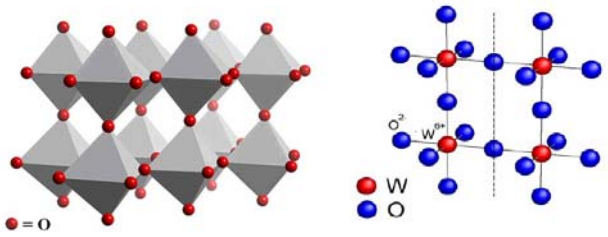

Figure 1. a) Polyhedral representation. b) Balls and sticks crystalline structure of WO_3. The atoms of W are located in the center of octahedra and oxygens in the vertices. Each oxygen forms one connection W-O-W.

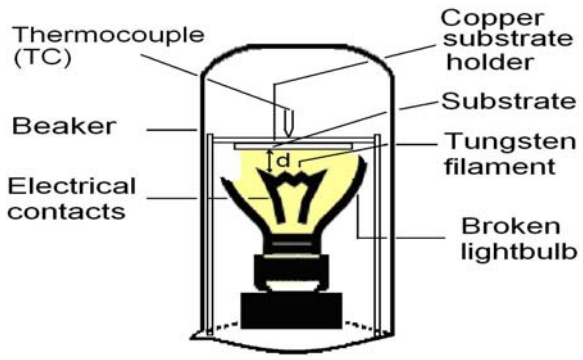

Figure 2. Experimental setting for the synthesis and condensation of WO_3 starting from a standard light bulb. Copper substrate holder of 50 x 30 x 7 mm^3; TC - thermocouple; filament-to-substrate separation: d = 30 mm.

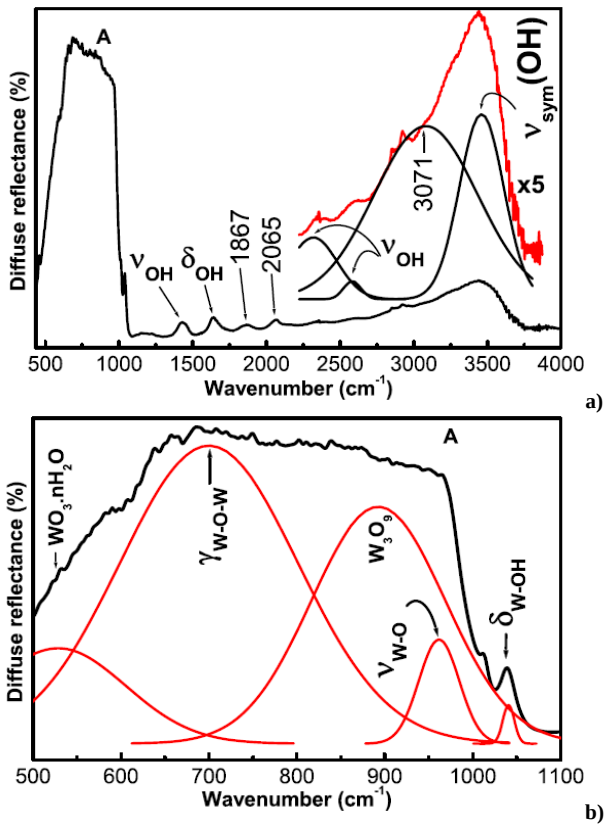

Figure 3. a) Diffuse Reflectance spectrum of a typical WO_3 film and b) It illustrates an amplification of peak A for showing its structure.

properties in a detailed manner and the results are presented.

2. General characteristics of WO_3 and transition metal oxides

An amorphous α–WO_3 film has a definite ionic and electronic conduction. It has large opened pore and it is constituted by clusters. The clusters are built from no more than 3-8 WO_6 –octahedra, linked together by corners or edges and in the complete structure of the film connected with one another by W-O-W bonds [9], see Fig. 1. The voids observed within the film are the result of random packing of the clusters and mostly give the open structure that is normally filled with molecular water taken from the air [8]. The presence of water is necessary to stabilize the microcrystalline structure of an α–WO_3 film with the opened pore structure. The ionic conduction of an α– WO_3 film is ensured by proton transport through channels or water bridges in pores, but the electronic conduction is done by the clusters linked together by W-O-W bonds. The binary W-O system is rather complex with a large number of phases. The most stable WO_3 phase at room temperature has a monoclinic structure, but this phase transforms to an orthorhombic or a tetragonal phase at higher temperatures. Many different structures of tungsten oxide clusters have been investigated [1]. The tungsten trioxide can crystallize in many polymorphs with various crystal structures [10]. Generally WO_3 and related electrochromic materials are divided into three main groups with regard to bulk crystalline structures: (i) Perovskite-like, such as WO_3, MoO_3, $SrTiO_3$; (ii) Rutile-like, TiO_2, MnO_2, VO_2, RuO_2, IrO_2 and RhO_2; (iii) Layer and block structures forming a somewhat undefined group, such as V_2O_5, Nb_2O_5.

3. The chemistry of the standard light bulb and synthesis of WO_3

It is very well known that even at normal conditions of operation, the standard light bulbs, 110 volts, have a time of average life of about 750 to 1000 h. That phenomenon is due to the evaporation of a small amount of the surface of the tungsten filament (Eq. 1) at the temperature and pressure to which the light bulb works, which thins the filament in certain sections and causes that changes the resistance in those points. Part of the formed tungsten steam is condensed by cooling with the inert gas that contains some light bulbs and/or by reduction of the temperature when extinguishing itself the light bulb. The black dust that is deposited in the inner wall of the bulb, which can be observed at first sight in the light bulbs which they have been some months of operation and in "the fused" light bulbs, is a direct test of it.

The second reason by that the filament is degraded and that closely is related to the previous one is that a series of chemical reactions to high temperature and low pressure happens, between the steam of formed tungsten and the

filling nitrogen or other originating gases of the air that cannot be evacuated in its totality within the light bulb. Of between those reactions, the main products are the tungsten oxide (Eq. 2) and the tungsten (VI) nitride (Eq. 3), which is disturbed with the water forming a little more WO_3 and ammonia, see Eqs. 4 and 5.

$$W_{(S)} \xrightarrow[110V,T\approx 3000^{o}C]{Ar/N_2 \ or \ P_{low}} W_{(g)} \quad (1)$$

$$2W_{(g)} + 3O_2 \longrightarrow 2WO_3 \quad (2)$$

$$W_{(g)} + N_2 \longrightarrow WN_2 \quad (3)$$

$$WN_2 + 3H_2O \xrightarrow[\Delta]{} WO_3 + 2NH_3 \quad (4)$$

$$NH_3 + H_2O \longrightarrow NH_4OH \quad (5)$$

4. Experiment details

The fact that light bulb blew is a disadvantage in the daily life, although the standard light bulbs are very cheap. In contrast, the intentional oxidation of the filament of a standard light bulb by electrical heating at 110 volts in presence of air is a very amazing phenomenon and it allows us to obtain tungsten (VI) oxide at a very low cost and with common materials. The WO_3 obtained from a single light bulb filament is enough to characterize the electrochromic compound by infrared and Raman spectroscopy.

Figure 2 depicts the experimental deposition setup that was designed in our laboratory for the synthesis of transition metal oxides. The tungsten filament is obtained broking the outline of glass bulb to uncover it. Then it is connected to an AC power supply to induce its resistivity heating. Oxygen is introduced to the growth chamber via an electronic mass flowmeter. Pressure measurements are made using a capacitance manometer. The chamber base pressure is the atmospheric pressure. In first instance we studied WO_3 in powder and after in thin films deposited in glass substrates.

The infrared spectroscopy analysis was performed using a Brucker Infrared Spectrometer Vertex 70 in the Diffuse Reflectance (DR) and Attenuated Total Reflection (ATR) modes. A ZnSe crystal in a single reflection ATR plate was used; the transmission percentage values of this kind of plate are greater than 25. Initially, ATR spectra were obtained for CA and PMMA in the solid state or as a film, and for the SP in a powder. Raman scattering experiments were performed at room temperature using the 6328 Å line of a He-Ne laser at normal incidence for excitation. The laser light was focused to a diameter of 6.0 μm at the sample using a 50x (numerical aperture 0.9) microscope objective. The nominal laser power used in these measurements was 20 mW. Care was taken to avoid the heating of the sample inadvertently to the point of changing its Raman spectrum. Scattered light was analyzed using a micro-Raman system (Lambram model of Dilor), a holographic notch filter made by Kaiser Optical System, Inc. (model superNotch-Plus), a 256x1024-pixel CCD used as detector cooled to 140 K using liquid nitrogen, and two interchangeable gratings (600 and 1800 g/mm). Typical spectrum acquisition time was limited to 60 s to minimize the sample heating effects discussed above. Absolute spectral feature position calibration to better than 0.5 cm^{-1} was performed using the observed position of Si which is shifted by 521.2 cm^{-1} from the excitation line.

Assignation of each vibrational mode is accomplished studying the behavior of the FTIR and Raman spectra with the excitation power. The wavenumber positions and the line width at half-maximum (FWHM) of each peak have been determined by a quantitative fit to the experimental FTIR and Raman spectra using a sum of Gaussian and Lorentzian line distributions, the dominant peaks were fit first and the additional peaks were added as necessary.

5. Results and discussion

The appearance of the reaction product makes suppose us that the main product of the reaction is the WO_3. The crystalline structure of this oxide is a three-dimensional adjustment (it is an oxopolianion) of WO_6 octahedra, in which the atoms of W are located in the center of the octahedra and oxygens are at the vertices, thus each oxygen is forming a connection W-O-W. In the infrared spectra of the crude of reaction, the observed absorption bands are due to the stretching of connections O-W-O. In order to remove some amount of a possible WN_2 formed as a byproduct, the crude one of reaction ~~it~~ was warmed up to water ebb tide during 10 minutes, later one filtered and it was dried to 105 °C during 1 h and one became to take the IR measurements but it was not observed changes that allowed us, by absence of peaks, to determine the bands corresponding to connections W-N.

WO_3 consists of packed corner-sharing WO_6 octahedra, contains 4 atoms and 6 fundamental normal modes of vibration. The observed vibration bands are mainly the fundamental vibrations of W═O, W-O and W-O-W chromophores. The local symmetry of the W═O chromophore allows the separation of normal modes according to the direction of their dynamic dipoles, helping the assignment of IR active vibrations. For molecular structure and orientation determination, the most relevant normal modes are the stretching vibrations (ν), in-plane bending vibrations (δ) and out-of plane wagging (γ) modes.

As it is known, the structure and components of the material dominate the properties of thin films. Both IR and Raman spectroscopy are very powerful tools to analyze the structure, phase and components of materials such as tungsten oxides. They are suitable to study the vibration and rotation of molecules. With these techniques, it is possible not only to identify different oxide phases but also to detect intercalated H_2O. The vibration spectroscopies play a key role in the characterization of EC films. Such studies allow obtaining fundamental information about WO_3 films for applications. In this section, an investigation

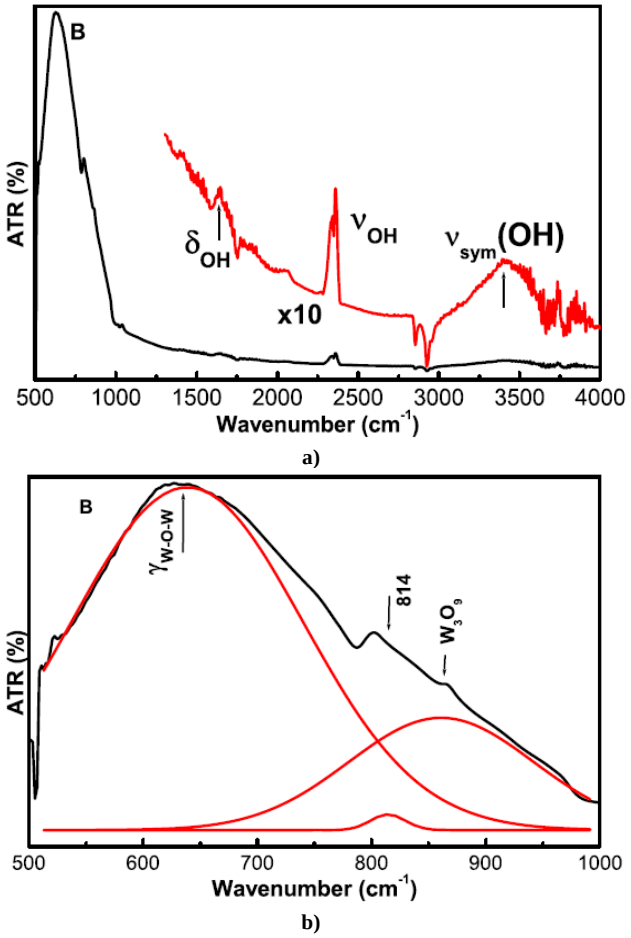

Figure 4. a) ATR spectrum of a typical WO_3 film deposited by resistive heating and b) It shows an amplification of the associated band to WO_3.

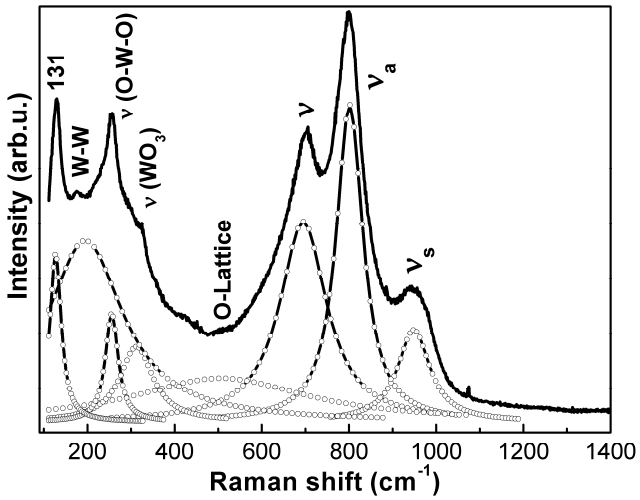

Figure 5. Raman spectrum of a typical WO_3 film deposited by resistive heating.

of Raman spectroscopy on tungsten oxide thin films is done.

Due to IR high sensitivity in the presence of the OH group, direct experimental proof of the presence of water in the films can be deduced from the IR spectra. This is important due to the role-played by water in the EC mechanism. IR spectra of α-WO_3 films and polycrystalline WO_3 are similar. Their maxima in the frequency range of deformation vibration (100-400 cm^{-1}) do not differ. The center of gravity for the IR absorption bands in this region is the same [9,11,12].

The diffuse reflectance spectrum of WO_3 deposited at RT and at –110 V bias is constituted with many bands in the region 1400-3600 cm^{-1}, see Fig. 3. The peaks located at the range 1100 to 3812 cm^{-1} are well resolved. These originated bands from moisture are assigned to ν(OH) and δ(OH) modes of adsorbed water. For the assigning of the peaks of the diffuse scattering spectrum were used the data of the table I. Especially from the peak sited at 1433 cm^{-1} with which is deduced that an OH group is strongly bonded to either water molecules or to surface oxygen atoms [11,13]. We find evidence for the formation of OH groups in the spectral range between 1400 and 3600 cm^{-1}. In the region of >3700 cm^{-1} the samples exhibit a very high transmittance due to a low absorption character.

The main tungsten (VI) oxide vibrations are found in the infrared regions of 1453-600 cm^{-1} and about of 3454 cm^{-1}, which correspond to tungsten-oxygen stretching, bending and lattice modes [14]. Here we find some relatively strong and weak bands at 528, 700, 670 893, 962 and 1041 cm^{-1}, see Fig. 3b. The 528 cm^{-1} band is assigned to the strong coupling of the oxide lattice in hydrated $WO_3 \bullet nH_2O$ material [15,16]. The 700 cm^{-1} band is assigned to the out of plane deformation W-O-W mode, when hydrogen is located at a coplanar square of oxygen atoms [17].

A relatively weak band at 1041 cm^{-1}, which is assigned to the plane deformational (bending) W-OH mode, was found. This peak at 1041 cm^{-1} is assigned to δ(OH) in W-OH group [15]. Because of the creation of weakly bonded W-OH groups is formed in the as-deposited film. In the frequency range from 400 to 1100 cm^{-1}, the shoulder around 962 cm^{-1} (W═O terminal modes of surface grains) [17] and W-O-W bridging mode 893 cm^{-1} [18].

Figure 4 shows the ATR spectrum, which presents fewer bands than the DR spectrum, but they confirm the later discussed. The six peaks sited at 639, 814, 861, 1649, 2360 and 3400 cm^{-1} that are associated at W-O-W [17], ν(W-O-W) [18], ν(W_3O_9) [19], (OH, H-O-H) [17,20], O-H [20] and W-OH…H_2O [17].

Since inorganic compounds have vibrational bands mainly below 1200 cm^{-1}, an investigation of Raman spectroscopy of WO_3 thin films was done in the range 100~1200 cm^{-1}. Bange [21] has studied vacuum deposited tungsten oxide films by mass spectroscopy. It was observed that the mass spectrum of the films consists of WO_2, WO_3, W_2O_6, W_3O_8 and W_3O_9. The WO_3 structure consists of an infinite number of packed corner-sharing $(WO_6)_6$-octahedra. To elucidate how many clusters are necessary to

Table 1. Summary of the IR assignment of the WO_3.

Group	**Wavenumber** (cm^{-1})	**[Reference]**	**Assignment**
W-OH···H_2O	3454	[14,17]	$\nu_{sym(OH)}$ -$\nu_{asym(OH)}$
-	3400	-	-
O-H	3071	[20]	ν_{OH}
-	2579		-
-	2312		-
-	2065		-
-	1867		
OH, H-O-H	1633 1649	[17,20]	(a) δ_{OH} in W-OH, (b) $\delta_{(OH\ O)}$
OH, W-O	1433	[11,13] [17]	ν_{OH}, δ_{OH} ν_{W-O}
W-OH	1041	[15]	δ_{W-OH}
W═O, W-O	962	[17]	ν_{W-O}
W-O-W	893	[18]	W_3O_9
	861	[19]	ν (W_3O_9)
	814	[18]	ν (W-O-W)
W-O-W	700	[17]	γ(W-O-W)
	639	[17]	γ(W-O-W)
O- Lattice	528	[15,16]	
W-O	417	[18]	δ_{W-O}

give the bulk properties, Nagai calculated the electronic structure of the clusters in various dimensions. Even an accumulation of 12 clusters is not sufficient to represent the bulk properties [22]. In the following section, the observed vibrational spectrum is described and discussed. To consolidate the observations made by the various research groups, values that fall in different frequencies were grouped together for simplicity. This is a reasonable way to present such data since one is dealing with solid-state spectroscopic measurements that show effects due to the oxygen stoichiometric variations, crystalline disorder, mixed phases, attainable signal-to-noise ratio, instrument calibration errors and variations in the technique. The assignment and comparison of the characteristic vibrations of the IR and Raman spectra are given in Tables I and II**.**

Raman spectrum of WO_3 film deposited at 300ºC is shown in Fig. 5, which is sited at range 90-1500 cm^{-1}. Raman bands of the transition metal (M) oxide in the range 950 - 1050 cm^{-1} can be assigned to a symmetric stretching mode of short terminal M=O bands, ν_s (M=O terminal). The bands in the range 750 - 950 cm^{-1} are attributed to either the antisymmetric stretch of M-O-M bonds (i. e., ν_{as} [M-O-M]) or the symmetric stretch of (-O-M-O-) bonds (i. e., ν_s [-O-M-O-]) [23]). The strongest peak located at 949 cm^{-1} belongs to ν_s (W=O terminal) of cluster boundaries [24]. The W=O terminal stretching belongs to the W-O bonds at the free surface of internal grains. This remarkable relative intensity of the double W=O bond, typical of non bridging oxygen, is caused by the absorbed water molecules and is frequently seen in sputtered or evaporated films deposited at lower temperatures [16].

The peak sited at 806 cm^{-1} is typical Raman peak of crystalline WO_3 (m-phase), which corresponds to the stretching vibrations of the bridging oxygen [25]. This peak is assigned to W-O stretching (ν), W-O bending (δ) and O-W-O deformation (γ) modes respectively [16, 26]. The peak at 695 cm^{-1} belongs to the O-W-O mode of WO_3•nH_2O [24]. The asymmetric band at 645 cm^{-1} is probably associated with stretching motions within the equatorial plane and is inside the range of 600 - 800 cm^{-1}. All the above discussions indicate that the clusters of the film are connected to each other by W-O-W or hydrogen bonds through water bridges with terminal W=O bonds at the surface of the clusters [26].

Since the W═O double bond is stronger than the W-O single bond, its vibration frequency is expected to be higher than that of the W-O bond. As it is known, there are some difference about the position of the W=O bond (range of 930-975 cm^{-1}). D. Gazzoli [27] indicated that the Raman positions depended on the tungsten content: the higher the W content, the higher the frequency at which the band appears and the removals of water causes a shift of the Raman bands to higher frequency.

Table 2. Summary of observed data of Raman for WO_3 ν_s = symmetric stretch; ν_a = anti symmetric stretch; ter. = terminal.

Raman (cm^{-1})	**[Reference]**	**Raman Groups & Assignment**
949	[24]	ν_s (W=O ter.)
806	[23,16,26]	ν_a (W-O-W)
695	[24]	ν (W_2O_6&W_3O_8)
518	[15,16]	O-Lattice
316	[12]	ν (WO_3)
256	[11,16]	ν (O-W-O) δ (O-W-O)
194	[21]	W-W
131	---	----

The sharp peak at 518 cm^{-1} is attributed at O-lattice. Besides, the Raman spectrum presents peaks at low wavenumbers. M. Regragui *et al.* [28] reported that they observed peaks in the range 90-280 cm^{-1}. Obviously, there is a group of peaks sited at 131, 194, 256 and 316 cm^{-1} in the Raman spectrum of Fig. 5. Most peaks below 200 cm^{-1} are attributed to lattice modes, whereas the mid and high frequency regions correspond to deformation and stretching modes, respectively. The sharp peaks at 256 and 316 cm^{-1} are assigned to the bending vibration δ(O-W-O) [11,16]. The Raman peak at 256 cm^{-1} is typical mode that indicates the crystalline quality of WO_3 film.

6. Conclusion

Starting from an electrical light bulb, tungsten (VI) oxide can be obtained, a material that has important technological applications. From the educative point of view, the synthesis of WO_3 by resistive heating of the tungsten filament of a center constitutes a simple and cheap spectacular experiment, which can be applied in diverse educative levels

Although apparently the method of synthesis by resistive heating does not seem to be very conventional, recently has been used for the synthesis of thin films of WO_3, applying a pure oxygen flow and using an electrical device a little more sophisticated than the one presented in this article.

References

[1] D. Manno, A. Serra, M.Di. Guilio, G. Micocci, A. Tepore, Thin Solid Films **324**, 44 (1998).
[2] S.K. Deb, Appl. Opt. **3J,** 192 (1969).
[3] C.G. Granqvist, Handbook of Inorganic Electrochromic Materials, Elsevier, Amsterdam, 1995.
[4] P. Cox, the Electronic Structure and Chemistry of Solids, Oxford University Press, Oxford, 1987.
[5] B.W. Faughnan, R.S. Crandall, Top. Appl. Phys. **40**, 181 (1980).
[6] S. Passerini, B. Scrosati, A. Gorenstein, A.M. Andersson, C.G. Granqvist, J. Electrochem. Soc. **136**, 3394 (1989).
[7] R. Sivakumar, A. Moses Ezhil Raj, B. Subramanian, M. Jayachandran, D.C. Trivedi, C. Sanjeeviraja, Mater. Res. Bull. **39**, 1479 (2004).
[8] K. Miyake, H. Kaneko, M. Sano, N. Suedomi, J. Appl. Phys. **55**, 274 (1984) 7.
[9] J. V. Gabrusenoks, P. D. Cikmach, A.R. Lusis, J. J. Kleperis and G. M. Ramans, Solid State Ionics **14**, 25 (1984).
[10] L. E. Depero, S. Groppelli, I. Natali-Sora, L. Sangaletti, G. Sberveglieri, E. Tondello, J. Solid State Chem. **121**, 379 (1996).
[11] A. Raougier, F. Portemer, A. Quede, M. EI Marssi, Appl. Surf. Sci. **153**, 1 (1999).
[12] L. Dixit, S. K. Kapoor, I. D. Singh and P. L. Gupta, Indian J. Phys. B **51**, 116 (1977).
[13] G. Atanassor, R. Thielsch, D. Popor, Thin Solid Films **223**, 288 (1993).
[14] P. Delichere, P. Falaras, M. Froment, A. Hugot-Le Goff, Thin Solid Films **161**, 35 (1988).
[15] C. J. Wright, J. Solid State Chem. **20**, 89 (1977).
[16] F. Daniel, B. Desbat, J. C. Lassegues, B. Gerand, M. Figlarz, J. Solid State Chem. **67**, 235 (1987).
[17] J. Pfeifer, Cao Guifang, P. Tekula-Buxbaum, B. A. Kiss, M. Farkas-Jahnke, and K. Vadasdi, J. Solid State Chem. **119**, 90 (1995).
[18] I. Hargittai, M. Hargittai, V. P. Spiridonov and E. V. Erokhin, J. Mol. Struct. **8**, 31 (1971).
[19] U. Opara Krasovec, A. Surca Vuk, B. Orel, Electrochimica Acta **46**, 1921 (2001).
[20] H. A. Willis, J. H. van der Maas and R. G. J. Miller, Laboratory Methods in Vibrational Spectroscopy, 3rd Edition, John Wiley & Sons: New York (1987).
[21] K. Bange, Sol. Ener. Mater. And Sol. Cell **58**, 1 (1999).
[22] C. Cantalini, H. T. Faccio, M. Pelino, Sensors and Actuators B **31**, 81 (1996).
[23] B. M. Weckhuysen, J.-M. Jehng, I. E. Wachs, J. Phys. Chem. B **104**, 7382 (2000).
[24] T. Kubo, Y.Nishikitani, J. Electrochem. Soc. **145**, 1729 (1998).
[25] P. Tagtstrom, U. Jansson, Thin Solid Films **352**, 107 (1999).
[26] Y. Shigesato, Y. Hayashi, A. Masui, T. Haranou, Jpn. J. Appl. Phys. **30**, 814 (1991).
[27] D. Gazzoli, M. Valigi, R. Dragone, A. Marucci and G. Mattei, J. Phys. Chem. B **101**, 11129 (1997).
[28] M.Regragui, M. Addou, A. Outzourhi, J. C. Bernede, Elb. EI Idrissi, E. Benseddik, A. Kachouane, Thin Solid Films **358**, 40 (2000).